



2 Development of a Model Framework for Terrestrial Carbon Flux Prediction: the Regional Carbon 3 and Climate Analytics Tool (RCCAT) Applied to Non-tidal Wetlands 4 Ashley Brereton^{1,2*}, Zelalem A Mekonnen¹, Bhavna Arora¹, William J. Riley¹, Kunxiaojia Yuan¹, Yi Xu², 5 Yu Zhang³, Qing Zhu¹, Tyler L. Anthony⁴, Adina Paytan² 6 * ashbre@lbl.gov: Corresponding author 7 Earth and Environmental Sciences Area, Lawrence Berkeley National Laboratory, Berkeley, CA, 8 USA1 9 Department of Earth and Planetary Sciences, University of California at Santa Cruz, Santa Cruz, 10 CA, USA² 11 Earth and Environmental Sciences Division, Los Alamos National Laboratory, Los Alamos, New 12 Mexico, USA³ 13 California Department of Water Resources, Sacramento, CA, USA⁴ 14 15 16 17 Abstract 18 Wetlands play a pivotal role in carbon sequestration but emit methane (CH₄), creating 19 uncertainty in their net climate impact. Although process-based models offer mechanistic 20 insights into wetland dynamics, they are computationally expensive, uncertain, and difficult to 21 upscale. In contrast, data-driven models provide a scalable alternative by leveraging extensive 22 datasets to identify patterns and relationships, making them more adaptable for large-scale 23 applications. However, their performance can vary significantly depending on the quality and 24 representativeness of the data, as well as the model design, which raises questions about their 25 reliability and generalizability in complex wetland systems. To address these issues, we present 26 a data-driven framework for upscaling wetland CO₂ and CH₄ emissions, across a range of 27 machine learning models that vary in complexity, validated against an extensive observational 28 dataset from the Sacramento-San Joaquin Delta. We show that artificial intelligence (AI) 29 approaches, including Random Forests, gradient boosting methods (XGBoost, LightGBM), 30 Support Vector Machines (SVM) and Recurrent Neural Networks (GRU, LSTM), outperform 31 linear regression models, with RNNs standing out, achieving an R2 of 0.72 for daily CO2 flux 32 predictions compared to 0.62 for linear regression, and an R² of 0.60 for CH₄ flux predictions 33 compared to 0.54 for linear regression. Interestingly, linear regression performed better than 34 random forest for methane flux, which highlights the necessity for comparison. Despite that, 35 interannual variability is less well captured, with annual mean absolute error of 193 gC m⁻² yr⁻¹ 36 for CO₂ fluxes and 11 gC-CH₄ m⁻² yr⁻¹ for CH₄ fluxes. By integrating vertically-resolved 37 atmospheric, subsurface, and spectral reflectance information from readily available sources,





the model identifies key drivers of wetland CO₂ and CH₄ emissions and enables regional upscaling. These findings demonstrate the potential of AI methods for upscaling, providing practical tools for wetland management and restoration planning to support climate mitigation

41 efforts.

42

43

44

45

46

47

48

49

50

51

52

53

54

55

56

57

58

59

60

61

62

63

64

65

66

67

68

69

70

71 72

73

74

75

76

77

78

3 1. Introduction

Wetlands provide a wide array of ecological, economic, and environmental benefits (Costanza et al., 2014). They play a crucial role in biodiversity conservation, water purification, flood control, and climate regulation (Grande et al., 2023; Sharma and Singh, 2021). Significant attention has been recently given to wetland restoration due to their ability to sequester carbon from the atmosphere (Lolu et al., 2020; Upadhyay et al., 2020). These ecosystems are highly effective at storing carbon in their soils because the anaerobic conditions in waterlogged soils suppress organic matter decomposition, allowing carbon to accumulate over time (Mitsch and Gosselink, 2015a). However, wetlands can also be significant sources of CH₄, a potent greenhouse gas (Brix et al., 2001), leading to potentially net positive effects of wetlands on climate warming. The most accurate way to determine the carbon balance in natural ecosystems is through direct and continuous measurements of carbon and GHG sources and sinks (Baldocchi et al., 2001). This involves monitoring carbon dynamics using techniques such as eddy covariance (EC) towers (Aubinet et al., 2012), soil carbon stock assessments (Harrison et al., 2011), and lateral carbon transport measurements (Ciais et al., 2008). However, these measurements are time-consuming to carry out, costly, and require specialized instruments and expertise, limiting their application to a few representative sites globally (Hill et al., 2017; Kumar et al., 2017). The Ameriflux network offers roughly 500 EC sites comprising about 3600 site years of data, monitoring carbon fluxes across various ecosystems such as forests, grasslands, and wetlands (Pastorello et al., 2020). Eddy-covariance site footprints range in scale and are typically determined by the sensor height and atmospheric turbulence (Chu et al., 2021). Data from these Ameriflux sites could potentially be upscaled and used for estimating fluxes from non-monitored sites to obtain regional assessments of carbon balance for various ecosystem types, including wetlands.

In this study, we focus on nontidal wetlands due to the presence of a cluster of EC towers in a small region located in the Sacramento-San Joaquin Delta, including three sites, each with over a decade of continuous data. Reported sequestration rates in wetlands vary widely, influenced by factors such as climate, vegetation, and management. For instance, reported sequestration rates range from as low as 26 gC m⁻² yr⁻¹ in boreal rain-fed bogs (Villa and Bernal, 2018) to as high as 797 gC m⁻² yr⁻¹ in constructed wetlands with emergent *Phragmites* in the Netherlands (de Klein and van der Werf, 2014). Similarly, temperate wetlands in central Ohio exhibit a wide range of carbon sequestration rates depending on vegetation: forested depressional wetlands dominated by *Quercus palustris* sequester up to 473 gC m⁻² yr⁻¹, while marshes dominated by *Typha* sequester around 210 gC m⁻² yr⁻¹ (Bernal and Mitsch, 2012). In Victoria, Australia, freshwater marshes show varying sequestration rates from 91 gC m⁻² yr⁻¹ in shallow marshes to 230 gC m⁻² yr⁻¹ in permanent open freshwater wetlands (Carnell et al., 2018). More relevant to



108

109

110

111

112

113

114



79 this study, in the San Francisco Bay-Delta region, nontidal managed wetlands dominated by 80 Schoenoplectus and Typha species sequester carbon at rates of approximately 355 ± 249 gC-81 CO2 m⁻² yr⁻¹. This estimate is based on direct calculations using Ameriflux data from sites with 82 over a decade of observations (US-Myb, US-Tw1, and US-Tw4). For this calculation we used 83 full-year annual averages and their corresponding standard deviation to the annual mean, to 84 highlight the significant inter-annual variability, with the standard deviation close to the mean. 85 The unit reported for these Delta sites is in gC-CO₂ m⁻² yr⁻¹, as the EC tower directly detects 86 CO₂ exchange, which is convenient for GHG assessment purposes. It is worth noting that, at 87 these sites, some years were a net CO₂ source, due to site-specific disturbances such as 88 caterpillar infestations, drought, or when vegetation cover was fully established (Anderson et al., 89 2018; Knox et al., 2017; Rey-Sanchez et al., 2021). See table S1 for more detailed information 90 and references therein.

91 Although CO2 balance (photosynthesis minus community respiration) is an important component of carbon sequestration, in many wetland systems sequestration benefits are counterbalanced 92 93 by CH₄ emissions, a potent greenhouse gas, with a warming potential 27 times higher than CO₂ 94 (Lee et al., 2023) that can often offset climate mitigation efforts. CH₄ emission rates also vary 95 substantially over time and across wetlands, from as low as 0.23 gC-CH₄ m⁻² yr⁻¹ in saltwater 96 zones of estuarine environments (Abril and Iversen, 2002) to as high as 270 gC-CH₄ m⁻² yr⁻¹ in 97 certain freshwater wetlands (Knox et al., 2021). For example, restored freshwater wetlands in 98 Maryland dominated by grasses and sedges emit around 142 gC-CH₄ m⁻² yr⁻¹ (Stewart et al., 99 2024). Tropical wetlands in Costa Rica exhibit some of the highest emissions, with isolated and 100 floodplain wetlands releasing between 220 and 263 gC-CH₄ m⁻² yr⁻¹ (Mitsch et al., 2013). The 101 San Francisco Bay-Delta wetlands that have high carbon sequestration rates also release CH₄ 102 at rates of 35 ± 13 gC-CH₄ m⁻² yr⁻¹ (direct measurements from the eddy covariance tower data 103 (Arias-Ortiz et al., 2021)). See table S2 for further information and reference therein. This dual 104 role of wetlands in both sequestering carbon and emitting CH₄ reveals the complex effect they 105 have on the global greenhouse gas balance. Therefore, integrating CO₂ and CH₄ emissions is 106 critical to assess the net climate benefits of wetland conservation and restoration initiatives.

To evaluate how wetlands contribute to the atmospheric radiation budget at larger scales, it is essential to quantify both GHG emissions and carbon sequestration, especially at sites where direct measurements are unavailable (Moomaw et al., 2018). Upscaling models serve this purpose by allowing estimation of sequestration and emission rates across larger spatial scales than those covered by the original data sources (Villa and Bernal, 2018) which provide GHG accounting and net climate benefit assessments for specific wetland sites (Nahlik and Fennessy, 2016). Moreover, it aids in targeting wetland restoration efforts that aim to optimize sequestration by identifying locations with the greatest potential for net carbon uptake.

Process-based models have traditionally been used to estimate sequestration and emissions (Mack et al., 2023; Zhang et al., 2002). Models such as DNDC (Li, 1996), DayCent (Parton et al., 1998), and *Ecosys* (Grant et al., 2017) have been applied to simulate biogeochemical processes in terrestrial ecosystems, including modeling CH₄ emissions, carbon balances, and soil carbon and nitrogen cycling (Grant and Roulet, 2002; Weiler et al., 2018; Zhang et al., 2002). While these models can elucidate the processes that play a role in carbon dynamics,





121 they require extensive mechanistic parameterization to accurately represent the interactions in 122 various ecosystems(Pastorello et al., 2020; Yin et al., 2023). This approach often necessitates 123 site-specific information and data collection, making implementation over vast areas challenging 124 (Saunois et al., 2024; Xu and Trugman, 2021). The extensive data needs associated with these 125 process-rich models showcase the need for alternative approaches that can effectively upscale 126 wetland emissions without such intensive resource demands. 127 Artificial Intelligence (AI) methods, such as machine learning and deep learning, have been 128 widely applied in ecological modeling in recent years, alongside long-term, large-scale data 129 collection efforts (Perry et al., 2022). Recent deep learning applications have demonstrated 130 success in capturing the complex dynamics of carbon and methane fluxes in these systems 131 (Ouyang et al., 2023; Yuan et al., 2022, 2024; Zou et al., 2024). The availability of open-source 132 modeling platforms like TensorFlow and PyTorch has made advanced computational 133 techniques, such as neural networks, more accessible, enabling the rapid development and 134 deployment of a range of specialized modeling tasks (Xu et al., 2021). Despite several recent 135 studies demonstrating the potential of machine learning for large-scale carbon cycling in 136 wetland ecosystems, this remains a relatively young field. Moreover, carbon dynamics in 137 wetland ecosystems are temporally variable and inherently nonlinear, making them particularly 138 well-suited for testing machine learning approaches (Arora et al., 2019, 2022). We therefore 139 emphasize the importance of evaluating and comparing various approaches within this domain 140 and their potential for large-scale assessment. 141 A pervasive challenge in model development is the ability to balance complexity with 142 generalizability. While more complex models can capture nonlinear relationships, they also 143 increase the risk of overfitting, where the model performs well in the testing, but poorly on new 144 conditions (Hastie, 2009; Tashman, 2000). Furthermore, it is also important to use a robust 145 validation framework. For the application of upscaling, it is important that the model is able to 146 extrapolate spatially. For this purpose, a leave-one-site-out (LOSO) validation approach is 147 typically carried out, whereby the models are trained on data that excludes a single site, with the 148 excluded site data saved for model testing (Bodesheim et al., 2018; Tramontana et al., 2016). It 149 is also important to avoid data leakage, where information from the training set inadvertently 150 appears in the testing set (Kaufman et al., 2012), a risk posed when splitting temporally 151 adjacent data points that are close in value, potentially inflating performance statistics (Bergmeir 152 and Benítez, 2012; Kaufman et al., 2012). For example, daily rates of change relative to a system where seasonal dynamics dominate, such as emissions of CH₄ emissions in vegetated 153 154 wetlands (Knox et al., 2021). 155 In this study, we introduce a model framework for coastal nontidal wetland CO2 and CH4 156 emissions using several 'off-the-shelf' models. These models are trained and validated against 157 observational data, and results are compared to find the most predictive model. The top 158 performing model is then used to upscale carbon sequestration and CH₄ emissions in nontidal 159 wetlands at regional scale. The San Francisco Bay-Delta serves as the area of interest, due to 160 its network of EC towers that have been operating for a relatively long time and relevance to 161 future wetland restoration efforts. We employ a suite of models, ranging widely in complexity: (1) 162 linear regression; (2) Random Forests (Breiman, 2001), an ensemble method that constructs



164

165

166

167

168

169

170

171

172

173

174

175

176

177178

179



multiple decision trees to reduce overfitting; (3) gradient boosting techniques such as LightGBM (Ke et al., 2017) and XGBoost (Chen and Guestrin, 2016), which are scalable tree boosting systems able to handle complex nonlinear relationships and variable interactions; (4) Support Vector Machines (SVM) (Cortes, 1995), a kernel-based technique that can approximate nonlinear boundaries between data points and (5) the Recurrent Neural Network (RNN) such as the Long Short-Term Memory (LSTM) neural network (Hochreiter, 1997), an advanced model designed to process sequential data and capture non-linear interactions over long-term dependencies. We also test a model with similar but simpler architecture, the Gated Recurrent Unit (GRU) (Chung et al., 2014), which uses fewer parameters. Linear regressions serve as a baseline to assess the applicability of the more sophisticated methods. Random Forests have been used to upscale northern wetland methane emissions (Peltola et al., 2019), gradient boosting methods have demonstrated success in ecological modeling (Ding, 2024; Räsänen et al., 2021; Zou et al., 2024), and LSTM neural networks have been successfully applied to model CO₂ and CH₄ fluxes in ecosystems (Yuan et al., 2022, 2024; Zou et al., 2024). Our proposed framework is designed to provide transparency, easy determination of model practicality and applicability, and contextualisation to model performances by comparing to a baseline model (i.e. linear regression).

180

181

189

190

191

192

193

194

195 196

197

198

199

2. Methods

- Our ultimate aim is to establish a robust modeling framework for estimating wetland carbon fluxes in sites that are not monitored. To achieve this, we compare a range of models, from simple linear regression to advanced recurrent machine learning neural networks. Since the goal is to predict unseen sites, we emphasize cross-site predictability by validating and testing the models at sites not included in training. Doing so ensures predictions are applicable beyond the training sites and addresses challenges often associated with model generalizability (Meyer and Pebesma, 2022). This strategy serves several purposes:
 - 1. **Performance Contextualization**: Starting with the simplest type of model provides a baseline for performance and helps evaluate the advantage (or lack thereof) for using more complex models.
 - 2. **Practicality and Transparency**: Advanced models may offer better performance but often require significant effort to set up and may lack interpretability. By comparing models of varying complexity using the same input data, we assess whether the added complexity is justified.
 - 3. **Feature Evaluation**: Training with different combinations of relevant features helps us to understand which features are dominating control, and the limitations of the data in terms of predictive capacity.

2.1 Model targets

The model targets two key variables: CO₂ (**FCO2**) and CH₄ (**FCH4**) surface emissions. Both variables follow a sign convention where positive values indicate emissions to the atmosphere



218

219

220

221

222

223

224

225

226

227

228

229

230

231

232



202 (source) and negative values indicate sequestration (sink). Both variables are available at half-203 hourly resolution through the Ameriflux database. 204 The models we developed all operate on a daily time scale, requiring target variables to be 205 aggregated to the daily time scale. This approach assumes that sub-daily variations have a 206 negligible non-linear contribution to longer time scales, an assumption supported by the dominant 207 seasonal signal typically observed in flux data from these systems (Knox et al., 2021). 208 These target variables could then be used to calculate annual NECB (Net Ecosystem Carbon 209 Balance; gC m⁻² yr⁻¹) and annual wetland net atmospheric radiative effect (FCO₂e (CO₂-equivalent 210 flux) $gCO_2e m^{-2} yr^{-1}$). The global warming potential (GWP) of non-fossil CH₄ is 27.2 as per the latest 211 IPCC assessment(Lee et al., 2023). For this study, we neglect contributions of lateral fluxes due to 212 data limitations, and that lateral transport at these sites is assumed to be negligible due to the 213 limited outflow from the wetlands (Miller et al., 2008). FCO2e is defined as annually averaged CO2 214 and CH₄ emissions, adjusted for the global warming potential (GWP) of each gas. A positive FCO₂e 215 indicates that the ecosystem is contributing positively to atmospheric warming, and vice versa. 216 Here we consider CO₂ and CH₄ emissions but neglect contributions from N₂O due to data

2.2 Region of interest

Myers et al., 2018).

The Sacramento-San Joaquin Delta was selected for this study due to its high density of EC towers and extensive long-term data. We selected sites for model training and validation where data was collected for at least a decade to capture interannual variability. Hence three restored wetland sites, US-Myb (Matthes et al., 2016), US-Tw1 (Valach et al., 2016), and US-Tw4 (Eichelmann et al., 2016) are selected in this study. While data from two other sites (i.e., US-Sne and US-Tw5) are available, the lack of sufficient temporal coverage and, in the case of US-Sne, not fully established vegetation cover, makes them less representative of a stable ecosystem. Focusing on sites with over a decade of continuous data allows for capturing long-term dynamics more effectively and provides sufficient time for the wetlands to reach a stable state. The dataset encompasses 35 full site-years of observations across the three sites within the Delta (Novick et al., 2018) (Table 2, Figure 1), with detailed mapping data sourced from the Ecoatlas Database (Workgroup, 2019) which provides land use and vegetation surveys across wetlands in California.

limitations and because N₂O emissions are considered negligible in Delta wetlands (Windham-

Table 2: Model training sites

Site Code	Site Name	Water Type	Salinity	Years of Data (Full)	Start Date
US-Myb	Mayberry Wetland	Non-Tidal	Fresh	13	2010
US-Tw1	Twitchell Wetland West Pond	Non-Tidal	Fresh	12	2011
US-Tw4	Twitchell Island East End Wetland	Non-Tidal	Fresh	10	2013





The sites are dominated by Tules (*Schoenoplectus*), Cattails (*Typha*), and invasive species such as *Phragmites*, which are perennial emergent plants well suited to wetland environments (López et al., 2016). The Delta itself is host to the largest estuarine system on the US Pacific coast, spanning approximately 3,000 km², and contains a diverse network of wetland systems. Historically, much of the area was drained and converted for agriculture (Laćan and Resh, 2016; Lund et al., 2010), but recent restoration efforts have reclaimed select portions of the landscape for environmental benefits.

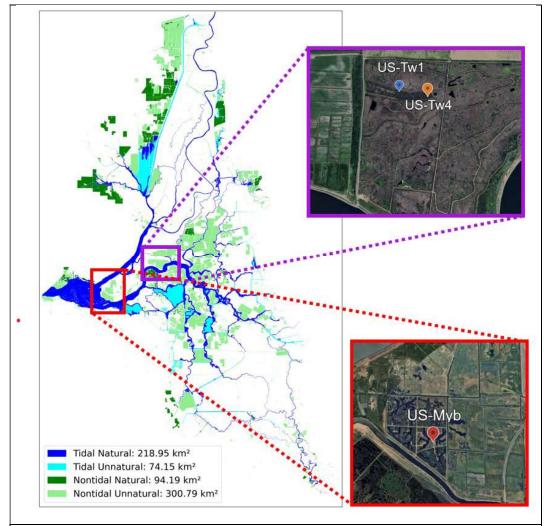


Figure 1: Map of the Sacramento-San Joaquin Delta's wetland system. The Eddy-covariance tower site locations outlined in Table 2 are shown in the red and purple boxes. Satellite image: © Google Earth, accessed 2024.





2.3 Model features

The application of this work focuses on upscaling carbon fluxes from similar wetlands at a regional scale. To achieve this, we aim to predict fluxes at unmonitored sites using widely available data that are expected to be key drivers of FCO2 and FCH4. Since site-level measurements from EC towers are not available at a larger spatial scale, we focus on ecosystem drivers that can be accessed across broader spatial extents.

The models utilize a comprehensive set of features from two readily accessible datasets: the Western Land Data Assimilation System (WLDAS) (Erlingis et al., 2021) and satellite-derived products from MODIS (Justice et al., 2002) (Supplementary Table S3). WLDAS provides high-resolution hydrological and meteorological data at 1-km spatial and daily temporal resolutions, spanning from 1980 to the present. Key variables include soil moisture, soil temperature, precipitation, solar radiation, and water table depth. MODIS complements these inputs with remote sensing data at a spatial resolution of 250–500 meters and temporal intervals ranging from 4 to 16 days, providing vegetation indices such as the Normalized Difference Vegetation Index (NDVI) and Leaf Area Index (LAI). The broad spatial and temporal coverage of these datasets enables upscaling across various regions. By relying on publicly available data sources, the framework remains practical and adaptable, facilitating rapid implementation with the appropriate training data.

2.4 Model suite

To evaluate ML model performance in calculating FCO2 and FCH4, we implemented a suite of seven models ranging from simple linear methods to more complex neural networks. These models have been used in various ecosystems to study fluxes and collectively represent a broad spectrum of methodological complexity. Table 3 summarizes the core characteristics and advantages of each approach.

Table 3: An overview of the models that are applied to wetland fluxes

Model Name	Category	Description	Key Strengths
Linear Regression	Regression	Fits a linear relationship between predictors and fluxes	Simple baseline, easily interpretable (Breiman, 2001)
Random Forest (Breiman, 2001)	Ensemble of Decision Trees	Aggregates multiple decision trees to enhance prediction stability	Robust to nonlinearity, reduces overfitting (Cortes, 1995)





Support Vector Machine (Cortes, 1995) (SVM)	Kernel-Based Method	Uses flexible kernels to find optimal separating hyperplanes	Effective in high dimensions, adaptable kernels (Ke et al., 2017)
LightGBM (Ke et al., 2017)	Gradient Boosting	Employs iterative boosting with efficient tree growth	Fast, memory- efficient, handles large datasets
XGBoost (Chen and Guestrin, 2016)	Gradient Boosting	Improves boosting with regularization and efficient computations	Manages outliers, handles sparse data well
LSTM Neural Network (Hochreiter, 1997)	Recurrent Neural Network	Captures temporal dependencies in sequential data inputs	Ideal for time- series, learns long- term patterns
GRU Neural Network (Chung et al., 2014)	Recurrent Neural Network	Similar to LSTM but streamlined with fewer parameters	Efficient temporal modeling, lower complexity

270

These models act to demonstrate a spectrum of model complexity and how that can be leveraged to improve flux prediction.

271272

273

274

275

276

277

278

279

287

2.5 Validation framework

To evaluate the models' ability to generalize across sites, we employed a Leave-One-Site-Out (LOSO) cross-validation strategy. In LOSO, we train the models on data from all but one site, and test the models on the excluded site. This approach is repeated for each site in the dataset and then aggregated, ensuring that there are no spatio-temporal connections between the training and testing data. While few models are immune to overfitting, this approach minimizes the risk of doing so.

An integral part of our modeling approach is the strategic selection of input features to optimize the model's performance. We perform this selection by first selecting features that are expected to be important, guided by mechanistic considerations of wetland processes gained from fieldwork and insights from mechanistic models (Table S3). Since the total number of possible feature combinations is too large for an exhaustive search, we adopt a feed-forward selection (**FFS**) strategy. This method begins with a single feature and iteratively adds features that most improves the model's performance based on a chosen statistic. At each step, we evaluate the model's

performance with each potential new feature and select the one that provides the greatest



323

324



288 improvement. This process continues until adding additional features no longer significantly 289 enhances the model's performance. By using this approach, we efficiently identify the most 290 influential predictors without the computational burden of testing all possible combinations. 291 2.6. Validation 292 293 As suggested above, each model was trained using data from two wetland sites and then 294 validated on the third. Although the number of sites was limited, each site offered over a decade 295 of observations accumulated to a daily time step, ensuring exposure to a range of 296 environmental conditions representative of the wetland type and regional climate. For each 297 excluded site, the model's predictions were compared against measured FCO2and FCH4. We 298 aggregated performance metrics (R2, Pearson correlation coefficient (r), and RMSE) across all 299 site predictions. This process was paired with the FFS method optimized to maximize R². 300 3. Results 301 3.1 Model Validation 302 303 We tested six modeling techniques of varying complexities (Table 3). Model performance scores 304 for daily predictions are shown in Figure 2, demonstrating that nearly all machine learning 305 models outperformed the linear regression baseline ($R^2 = 0.62$ for FCO2 and $R^2 = 0.54$ for 306 FCH4). For FCO2, LSTM and GRU achieved the highest R² values (0.71 and 0.70, 307 respectively), outperforming other methods. A similar result was found for FCH4, with LSTM and 308 GRU both scoring R2 of 0.60. These results suggest that deep learning models can provide tangible benefits over linear regression methods for upscaling flux predictions. The LSTM model 309 310 was selected for upscaling in this study as it scored highest consistently, though other ML 311 models scored comparably, so we do not assert it as definitively the best model. 312 The feature selection process had access to 26 environmental features from WLDAS and 8 313 features from MODIS (see table S3 for full details). These variables encompass a wide range of 314 atmospheric, soil, and vegetation characteristics, such as precipitation, temperature, soil 315 moisture, and spectral indices, key environmental drivers known to influence carbon and 316 methane flux dynamics (Mitsch and Gosselink, 2015b). Results revealed that model 317 performance plateaued after including 4 features, meaning that only a small subset of predictors were needed to maximize predictive skill. Notably all ML models, regardless of complexity, 318 319 selected the same initial feature for both FCO2 and FCH4, which highlights temperature as a 320 dominant environmental driver. As shown in Table 4 for the LSTM case, temperature-related 321 variables emerged as the first selected feature for both FCO2 (Air Temperature) and FCH4

(Canopy Temperature) predictions, illustrating the importance of temperature in driving

ecosystem activity. As an aside, while temperature variables may be most significant in the first

step, many other features scored comparably. The subsequent inclusion of hydrological and





spectral reflectance variables led to modest improvements in R² values, which is also mirrored by improvements in RMSE and r.

Table 4: Feed-forward feature selection process.

Target Variable	Step	Chosen Feature	R²	RMSE	r
FCO2	1	Air Temperature	0.66	1.62	0.82
FCO2	2	Water Table Depth	0.68	1.57	0.83
FCO2	3	Bare Soil Evaporation	0.70	1.54	0.84
FCO2	4	Blue Reflectance	0.71	1.50	0.85
FCH4	1	Canopy Temperature	0.52	0.054	0.73
FCH4	2	Near-Infrared Reflectance	0.58	0.051	0.76
FCH4	3	Total Evapotranspiration	0.60	0.050	0.77

Figure 3 shows both FCO2 and FCH4 results, including time series and scatter plots comparing predictions to observations. Overall, the predicted values track the observations reasonably well. For FCO2, predictions tended to regress toward the mean, underestimating peak emissions at local maxima and overestimating at local minima. The ML models also displayed less interannual variability than the observations, common in machine learning approaches (Ouyang et al., 2023). For wetlands, this is likely due to limited subsurface process information included in the machine learning models. Still, the scatter plot shows strong performance for FCO2 (r = 0.84, R^2 = 0.71, RMSE = 1.49 gC-CO₂ m^{-2} day⁻¹), despite a noticeable spread around the 1:1 line.

FCH4 predictions exhibited similar behavior, with lower interannual variability than the observations. At the US-Myb site, for example, observed FCH4 were initially high (aside from the first year, when vegetation cover had yet to be fully established) but declined over time, stabilizing at lower values. The ML models captured this shift to some extent, predicting higher fluxes early in the time series and then modulating to lower levels later on. However, predictions did not fully replicate the magnitude of the observed downward annual trend, introducing bias

https://doi.org/10.5194/egusphere-2025-361 Preprint. Discussion started: 1 April 2025 © Author(s) 2025. CC BY 4.0 License.



349

351

354

355

356

357

358

359

360

361

362

363

364

365

366

367

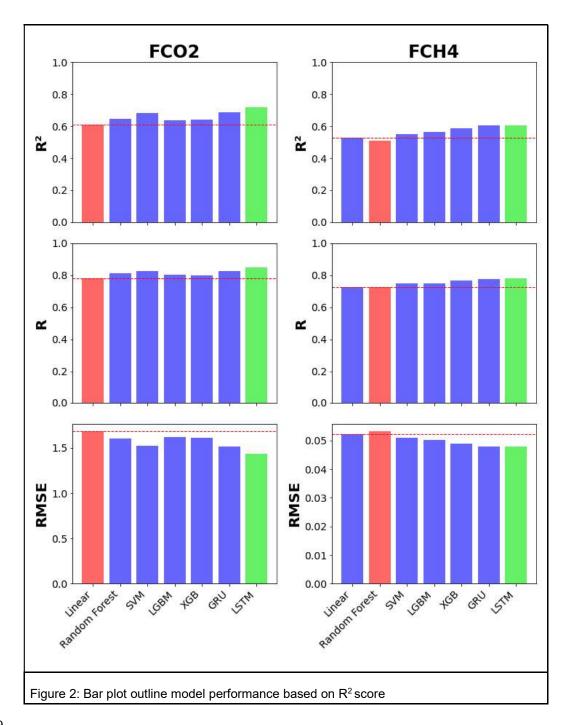


345 into the scatter plots at higher and lower extreme values. This phenomenon is known as 346 regression to the mean, observed in similar machine learning studies (Ouyang et al., 2023). 347 Consequently, the FCH4 model performance was weaker than the FCO2 model (R2 = 0.61, r = 348 0.78, RMSE = 0.05 g C-CH4 m⁻² day⁻¹), indicating that the processes controlling FCH4 in vounger wetlands like US-Mvb may require more detailed subsurface information (such as soil 350 organic C, oxygen, or redox information) to be accurately modeled. The annual bar plots presented in Figure 4 highlight the model's difficulty in capturing the 352 interannual variability of carbon fluxes across the study sites. While the average FCO2 and 353

FCH4 predictions are generally aligned with observed average values with small overall mean bias, the model struggles to reproduce the observed year-to-year variability. Although direct subsurface measurements are available at certain sites, at the regional scale their limited spatial and temporal coverage currently limits integration into models designed for regional upscaling over inter-annual timescale. For example, while spatial maps of wetland soil organic carbon exist (Uhran et al., 2022), using only three sites for training purposes would provide just three corresponding data points, limiting model training. The LOSO validation approach revealed that deep learning models, particularly LSTM and GRU, consistently outperformed traditional linear regression and other machine learning methods for both FCO2 and FCH4 predictions. While nonlinear models demonstrated clear advantages, the magnitude of improvement was relatively modest, reflecting the inherent challenges of capturing site-specific inter-annual dynamics of wetland emissions. To improve model performance, additional techniques such as feature transformations or attention mechanisms could be implemented. However, the primary goal of this model suite is to ensure reproducible results with 'off-the-shelf' models, which serves as a foundation for more advanced, nuanced approaches.









374

375



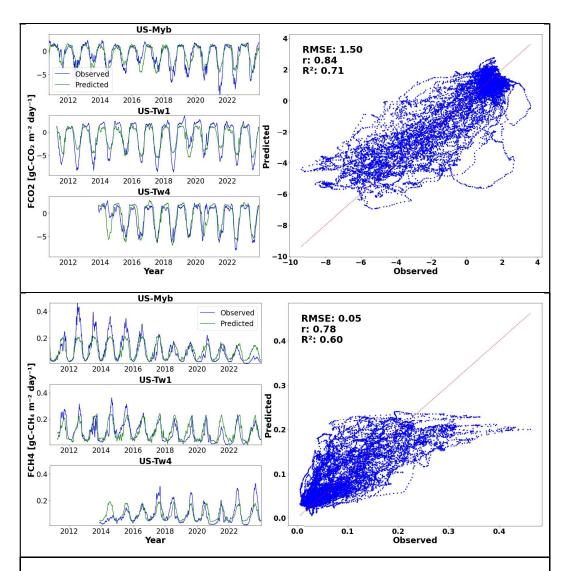


Figure 3: Time-series plots (left) of observed (blue) and predicted (green) FCO2 and FCH4 fluxes for US-Myb, US-Tw1, and US-Tw4. The scatter plot (right) compares observed vs. predicted values across all sites, with a 1:1 reference line (red dashed) and overall performance metrics (RMSE, r, R²) displayed in the upper-left corner.





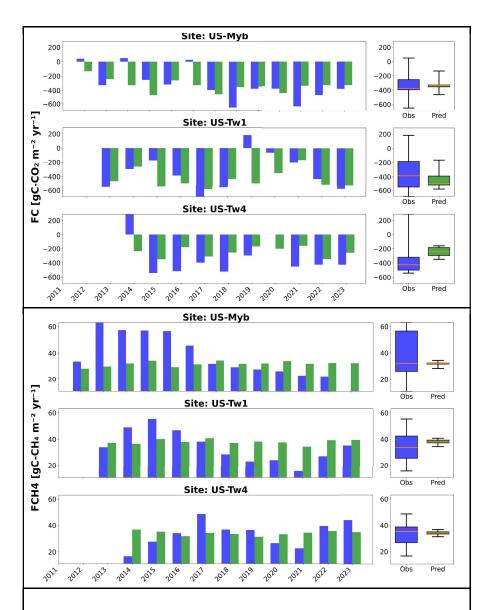


Figure 4: Annual Observed and Predicted FCO2 and FCH4 Across Three Wetland Sites. Aggregated statistics for all sites are as follows: For **FCO2**, the Mean Absolute Error (MAE) is **193 gC m**⁻² **yr**⁻¹ and the Mean Bias Error (MBE) is **-10 gC m**⁻² **yr**⁻¹. For **FCH4**, MAE is **11 gC-CH₄ m**⁻² **yr**⁻¹ and the MBE is **-2 36gC-CH₄ m**⁻² **yr**⁻¹.





3.2. Model Application: Upscaling

three sites for upscaling.. The Sacramento-San Joaquin Delta contains roughly 700km² of wetland area, including tidal and nontidal regions. The upscaling domain encompasses approximately 25 km² of nontidal wetlands in the region, dominated by vegetation types relevant to the training sites, specifically Tules, Cattails, and Phragmites. The assumption is that the training sites used in this study are representative of the broader conditions in the Delta, but we acknowledge that local variability in carbon dynamics, such as those caused by microclimates prevalent in the area, may not be fully captured during the ML model training. Improvements to the model might be achieved if additional site data covering a wider range of environmental conditions were incorporated. The feature data used to optimize the model were spatially interpolated onto the regional model grid and the model applied to yield flux estimations. Although relatively modest in spatial extent, these wetlands are of particular interest given their role in carbon sequestration and potential climate mitigation and as targets for conservation and restoration.

After selecting LSTM as the model of choice, it was retrained using all available data from the

Figure 5 displays spatial maps of annual flux estimates of Net Ecosystem Carbon Balance (NECB), methane flux (FCH4), and the CO₂ equivalent flux rate (FCO2e) in the study domain. The results show that carbon sequestration, indicated by negative NECB (green) values, are notably stronger in the more northern parts of the domain, which is likely driven by air temperature (dominant feature), with this region of California being subject to distinctive microclimates. In contrast, FCH4 shows a comparatively uniform spatial pattern, which was also observed in the model validation. Similar to NECB, the FCO2e distribution shows strong latitudinal dependence, with a net CO2e sink in northern zones and a tendency toward emissions in the southern portion of the study area, though localized heterogeneity exists.

Figure 6 shows averaged fluxes in the upscaling domain over the full study period. The results highlight the Delta as an overall carbon sink, with NECB averaging approximately -380 gC m⁻² yr⁻¹, indicating persistent sequestration across multiple years. CH₄ fluxes average 28 gC-CH₄ m⁻² yr⁻¹, and shows little spatial variability. Values are consistent with those previously reported in the region (Arias-Ortiz et al., 2021). Integrating these fluxes into a CO₂-equivalent metric, this regional wetland system remains a net sink of CO₂e, with approximately 400 gCO₂e m⁻² yr⁻¹ sequestered on average in the upscaling domain.





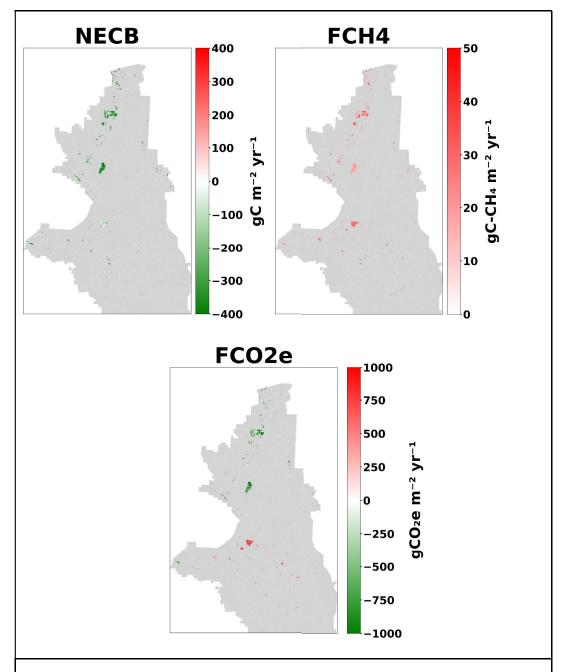


Figure 5: Spatial maps of the average annual fluxes across the Delta region. NECB (left) displays carbon sequestration. FCH4 (center) highlights CH_4 emissions. FCO2e (right) integrates CO_2 and CH_4 fluxes weighted by radiative forcing. Green indicates net sinks and red indicates net emissions to the atmosphere.





412

413

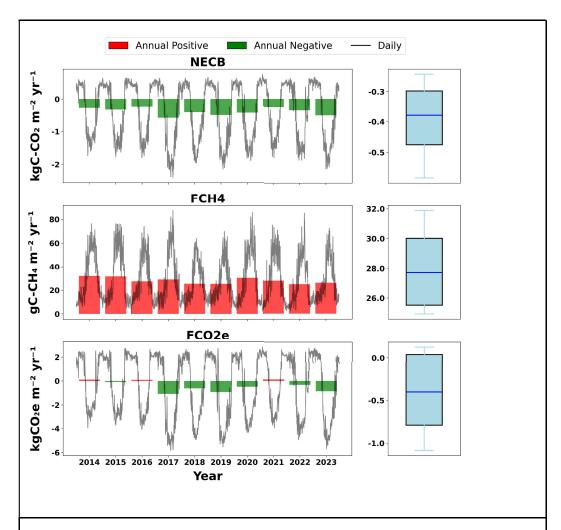


Figure 6: Bar plots and box plots of annual NECB, FCH4, and FCO2e fluxes, which have been spatially integrated over the study region, a total of 25 km² total land area vegetated primarily by Tules, but also Cattails and Phragmites. The left column shows annual fluxes for each year, with negative fluxes in green and positive fluxes in red. Daily fluxes, aggregated to annual totals, are overlaid as black lines. The right column shows box plots summarizing the distribution of annual fluxes, highlighting the range, median (blue line), and





spread of values. Each row represents a different flux variable: (a) NECB, (b) FCH4, and (c) FCO2e.

415

416

417

418

4. Discussion

419 This study demonstrates the development and evaluation of a data-driven framework to upscale 420 terrestrial CO2 and CH4 flux estimates for non-tidal wetlands in the Sacramento-San Joaquin

421 Delta. By systematically comparing models of varying complexity, including linear regression,

422 ensemble methods, gradient boosting algorithms, and recurrent neural networks (RNNs), we

423 presented a transparent assessment of model performance. The goals were to identify the 424 model that best predicts CO₂ and CH₄ fluxes and critically appraise whether incremental

425 complexity is justified by improvements in predictive capacity. Relevant cited works have

426 included many different machine learning approaches for predicting emissions. This work aims

427 to unify modelling efforts by establishing a standard framework for developing robust data-

428 driven models, particularly for upscaling purposes.

429 Our results indicate that non-linear and more advanced models generally outperformed simple

430 linear regression approaches. Among all tested models, the Long Short-Term Memory (LSTM)

431 and Gated Recurrent Unit (GRU) neural networks provided the highest overall skill in predicting

432 both CO₂ and CH₄ fluxes at daily timescales. This improvement was marginal but consistent,

433 supporting the notion that time-series models, which inherently capture temporal dependencies

434 and non-linearities, can provide tangible benefits over linear methods and traditional machine

435 learning algorithms.

436 However, while these deep learning models performed best, the performance gains were not as

437 large as might be expected given their significantly higher complexity and computational

438 demands. Similar outcomes have been noted in other ecological modeling applications, where

439 advanced machine learning methods yield improvements that are statistically significant yet

440 modest in terms of performance gains relative to linear models (Oh et al., 2022; Wood, 2022).

441 The deep learning models provided reasonable estimates of daily fluxes but struggled to

442 replicate the full range of interannual variability observed in the field measurements, which is a

443 common issue for data-driven models in this field (Nelson et al., 2024). This limited ability to

444 capture long-term trends and extremes mirrors common challenges in machine learning-based

445 modeling, where the absence of explicit mechanistic understanding limits extrapolation beyond

446 the conditions represented in the training data. The difficulty in reproducing interannual

447 fluctuations was particularly evident for CH4 fluxes, an outcome consistent with the high spatial

448 and temporal complexity of CH₄ cycling in wetland environments and the limited availability of





449 subsurface parameters (e.g., oxygen concentration, redox conditions, substrate availability) that 450 drive CH₄ production. This may not be surprising as the number of annual cycles available in 451 the training set was only 35 years. 452 The observed regression to the mean and the reduced dynamic range in model predictions may 453 reflect insufficient representation of key environmental drivers in the feature set or inadequate 454 temporal coverage and variability in the training data. While publicly available datasets such as 455 WLDAS and MODIS were effective at providing spatially and temporally comprehensive inputs, 456 the lack of direct subsurface and soil biogeochemical measurements likely limited the model's 457 ability to capture critical internal processes that are likely causing the observed differences 458 between years. Although the feed-forward selection process for the model features had access 459 to an extensive pool of relevant features, results indicated that only a small subset of features 460 was necessary to maximise performance. This suggests that, while there are many features that 461 control CO2 and methane, their contribution to predictive accuracy may be redundant or 462 captured indirectly by other variables. The exclusion of particular features, such as the water 463 table depth for FCH4, illustrates the trade-off between mechanistic intuition and data-driven 464 optimization. Strong correlations between features and limited independent variability can lead 465 to features being left out that would typically be considered ecologically relevant. 466 After applying the chosen model (LSTM) to calculate CO₂ and CH₄ fluxes, we estimated NECB 467 and CO₂-equivalent fluxes for similar wetland settings across the Delta region. The results show 468 spatial heterogeneity and pinpoint regions that act as stronger net carbon sinks, as well as 469 areas where CH₄ emissions may offset climate benefits of net carbon sequestration. Such 470 insights support targeted conservation and restoration strategies aimed at maximizing net 471 carbon sequestration benefits, facilitating ongoing efforts to restore and manage wetlands to 472 contribute to net-zero emission goals. 473 A key advantage of the chosen approach is its reliance on readily available, open-source data 474 streams and standard computational resources. The framework can be deployed efficiently 475 without specialized hardware, making it accessible to resource-limited organizations, 476 practitioners, and researchers. 477 The primary objectives of this study were to identify a suitable model, contextualize model 478 performance by comparing to a baseline linear regression, and highlight trade-offs between 479 complexity, interpretability, and accuracy. By explicitly testing multiple models ranging from 480 simple linear regressions to advanced recurrent neural networks, we demonstrated that 481 complexity alone does not guarantee a substantial increase in predictive power. Instead, 482 complexity should be adopted judiciously, based on the magnitude of performance gains, the 483 cost of model implementation, and the level of interpretability. 484 We suggest that future modeling efforts should focus on deriving mechanistically relevant 485 predictors (Ouyang et al., 2023), and incorporating hybrid modeling approaches (Yao et al., 486 2023) that combine the strengths of process-based and machine learning methods. Attention 487 mechanisms (Yuan et al., 2022), advanced architectures (e.g., Transformers (Vaswani, 2017)),





488 or physics-informed machine learning (Raissi et al., 2019) may also help address model 489 performance limitations. 490 5. Conclusions 491 492 493 This study provides a transparent, methodical demonstration of an artificial intelligence 494 approach to modeling wetland carbon dioxide (CO₂) and methane (CH₄) emissions, using a 495 suite of "off-the-shelf" tools and establishing a standardized benchmarking protocol for model 496 performance evaluation. In the study region (the Sacramento-San Joaquin Delta), inter-model 497 comparisons revealed modest but appreciable performance differences when comparing 498 advanced models with a linear regression baseline. While there are tangible benefits to 499 employing machine learning for these purposes, it is likely that the gap between simpler models 500 and more sophisticated models will widen as data quantity and quality continues to increase. 501 Ultimately, this study lays the groundwork for regional scale model benchmark testing, 502 facilitating the development of more advanced modeling approaches that can guide wetland 503 management, restoration planning, and climate mitigation strategies. 504 Code and data availability 505 506 The current version of the RCCAT model is available on GitHub at 507 https://qithub.com/ashbre2/RCCAT under the MIT License. The exact version of the model 508 used to produce the results presented in this paper has been archived on 509 Zenodo under https://doi.org/10.5281/zenodo.14933820 (Brereton, 2025) 510 **Author contributions** 511 AB developed the model, performed the analysis, and led the writing of the manuscript. ZM, BA, 512 AP, WR, and KY contributed to model development and provided expertise in carbon flux 513 modeling. QZ contributed expertise in machine learning methods. TA provided domain-specific 514 knowledge of the region of interest. YZ and YX contributed expertise in hydrological processes. 515 All co-authors reviewed, provided input on the manuscript drafts, and approved the final version. 516 Competing interests 517 The authors declare that they have no conflict of interest. **Acknowledgements** 518 519 This research was supported by funds from the UC National Laboratory Fees Research 520 Program (LFRP) of the University of California, Grant Number L22CR4529. We thank OpenAI





- and ChatGPT for help with wording and coding assistance, which accelerated progress
- 522 significantly.

- 525 Abril, G. and Iversen, N.: Methane dynamics in a shallow non-tidal estuary (Randers Fjord,
- 526 Denmark), Mar. Ecol. Prog. Ser., 230, 171–181, 2002.
- 527 Anderson, M., Gao, F., Knipper, K., Hain, C., Dulaney, W., Baldocchi, D., Eichelmann, E.,
- 528 Hemes, K., Yang, Y., and Medellin-Azuara, J.: Field-scale assessment of land and water use
- 529 change over the California Delta using remote sensing, Remote Sens., 10, 889, 2018.
- Arias-Ortiz, A., Oikawa, P. Y., Carlin, J., Masqué, P., Shahan, J., Kanneg, S., Paytan, A., and
- 531 Baldocchi, D. D.: Tidal and Nontidal Marsh Restoration: A Trade-Off Between Carbon
- 532 Sequestration, Methane Emissions, and Soil Accretion, J. Geophys. Res. Biogeosciences, 126,
- 533 e2021JG006573, https://doi.org/10.1029/2021JG006573, 2021.
- Arora, B., Wainwright, H. M., Dwivedi, D., Vaughn, L. J., Curtis, J. B., Torn, M. S., Dafflon, B.,
- 535 and Hubbard, S. S.: Evaluating temporal controls on greenhouse gas (GHG) fluxes in an Arctic
- tundra environment: An entropy-based approach, Sci. Total Environ., 649, 284–299, 2019.
- 537 Arora, B., Briggs, M. A., Zarnetske, J. P., Stegen, J., Gomez-Velez, J. D., Dwivedi, D., and
- 538 Steefel, C.: Hot Spots and Hot Moments in the Critical Zone: Identification of and Incorporation
- 539 into Reactive Transport Models, in: Biogeochemistry of the Critical Zone, edited by: Wymore, A.
- 540 S., Yang, W. H., Silver, W. L., McDowell, W. H., and Chorover, J., Springer International
- 541 Publishing, Cham, 9–47, https://doi.org/10.1007/978-3-030-95921-0 2, 2022.
- 542 Aubinet, M., Vesala, T., and Papale, D.: Eddy covariance: a practical guide to measurement and
- 543 data analysis, Springer Science & Business Media, 2012.
- 544 Baldocchi, D., Falge, E., Gu, L., Olson, R., Hollinger, D., Running, S., Anthoni, P., Bernhofer, C.,
- 545 Davis, K., and Evans, R.: FLUXNET: A new tool to study the temporal and spatial variability of
- 546 ecosystem-scale carbon dioxide, water vapor, and energy flux densities, Bull. Am. Meteorol.
- 547 Soc., 82, 2415–2434, 2001.
- 548 Bergmeir, C. and Benítez, J. M.: On the use of cross-validation for time series predictor
- 549 evaluation, Inf. Sci., 191, 192-213, 2012.
- Bernal, B. and Mitsch, W. J.: Comparing carbon sequestration in temperate freshwater wetland
- 551 communities, Glob. Change Biol., 18, 1636–1647, https://doi.org/10.1111/j.1365-
- 552 2486.2011.02619.x, 2012.
- 553 Bodesheim, P., Jung, M., Gans, F., Mahecha, M. D., and Reichstein, M.: Upscaled diurnal
- 554 cycles of land-atmosphere fluxes: a new global half-hourly data product, Earth Syst. Sci. Data,
- 555 10, 1327–1365, 2018.
- 556 Breiman, L.: Random Forests, Mach. Learn., 45, 5–32,
- 557 https://doi.org/10.1023/A:1010933404324, 2001.
- 558 Brereton, A. Regional Carbon Climate Analytics Tool (RCCAT), version 1.0.0, Zenodo,





- 559 https://doi.org/10.5281/zenodo.14933820, 2025.
- 560 Brix, H., Sorrell, B. K., and Lorenzen, B.: Are Phragmites-dominated wetlands a net source or
- net sink of greenhouse gases?, Aquat. Bot., 69, 313–324, 2001.
- 562 Carnell, P. E., Windecker, S. M., Brenker, M., Baldock, J., Masque, P., Brunt, K., and
- 563 Macreadie, P. I.: Carbon stocks, sequestration, and emissions of wetlands in south eastern
- 564 Australia, Glob. Change Biol., 24, 4173–4184, https://doi.org/10.1111/gcb.14319, 2018.
- 565 Chen, T. and Guestrin, C.: XGBoost: A Scalable Tree Boosting System, in: Proceedings of the
- 566 22nd ACM SIGKDD International Conference on Knowledge Discovery and Data Mining, KDD
- 567 '16: The 22nd ACM SIGKDD International Conference on Knowledge Discovery and Data
- 568 Mining, San Francisco California USA, 785–794, https://doi.org/10.1145/2939672.2939785,
- 569 2016.
- 570 Chu, H., Luo, X., Ouyang, Z., Chan, W. S., Dengel, S., Biraud, S. C., Torn, M. S., Metzger, S.,
- 571 Kumar, J., and Arain, M. A.: Representativeness of Eddy-Covariance flux footprints for areas
- 572 surrounding AmeriFlux sites, Agric. For. Meteorol., 301, 108350, 2021.
- 573 Chung, J., Gulcehre, C., Cho, K., and Bengio, Y.: Empirical Evaluation of Gated Recurrent
- Neural Networks on Sequence Modeling, https://doi.org/10.48550/arXiv.1412.3555, 11
- 575 December 2014.
- 576 Ciais, P., Borges, A. V., Abril, G., Meybeck, M., Folberth, G., Hauglustaine, D., and Janssens, I.
- 577 A.: The impact of lateral carbon fluxes on the European carbon balance, Biogeosciences, 5,
- 578 1259–1271, 2008.
- 579 Cortes, C.: Support-Vector Networks, Mach. Learn., 1995.
- 580 Costanza, R., De Groot, R., Sutton, P., Van der Ploeg, S., Anderson, S. J., Kubiszewski, I.,
- 581 Farber, S., and Turner, R. K.: Changes in the global value of ecosystem services, Glob.
- 582 Environ. Change, 26, 152–158, 2014.
- 583 DeLaune, R. D. and Pezeshki, S. R.: The role of soil organic carbon in maintaining surface
- 584 elevation in rapidly subsiding US Gulf of Mexico coastal marshes, Water Air Soil Pollut. Focus,
- 585 3, 167–179, 2003.
- 586 Ding, H.: Establishing a soil carbon flux monitoring system based on support vector machine
- 587 and XGBoost, Soft Comput., 28, 4551–4574, 2024.
- 588 Eichelmann, E., Shortt, R., Knox, S., Sanchez, C. R., Valach, A., Sturtevant, C., Szutu, D.,
- 589 Verfaillie, J., and Baldocchi, D.: AmeriFlux AmeriFlux US-Tw4 Twitchell East End Wetland,
- 590 Lawrence Berkeley National Laboratory (LBNL), Berkeley, CA (United States ..., 2016.
- 591 Erlingis, J. M., Rodell, M., Peters-Lidard, C. D., Li, B., Kumar, S. V., Famiglietti, J. S., Granger,
- 592 S. L., Hurley, J. V., Liu, P., and Mocko, D. M.: A High-Resolution Land Data Assimilation
- 593 System Optimized for the Western United States, JAWRA J. Am. Water Resour. Assoc., 57,
- 594 692–710, https://doi.org/10.1111/1752-1688.12910, 2021.
- 595 Grande, E., Seybold, E. C., Tatariw, C., Visser, A., Braswell, A., Arora, B., Birgand, F., Haskins,
- 596 J., and Zimmer, M.: Seasonal and tidal variations in hydrologic inputs drive salt marsh





- 597 porewater nitrate dynamics, Hydrol. Process., 37, e14951, https://doi.org/10.1002/hyp.14951,
- 598 2023.
- 599 Grant, R. F. and Roulet, N. T.: Methane efflux from boreal wetlands: Theory and testing of the
- 600 ecosystem model Ecosys with chamber and tower flux measurements, Glob. Biogeochem.
- 601 Cycles, 16, https://doi.org/10.1029/2001GB001702, 2002.
- 602 Grant, R. F., Mekonnen, Z. A., Riley, W. J., Arora, B., and Torn, M. S.: 2. Microtopography
- 603 determines how CO2 and CH4 exchange responds to changes in temperature and precipitation
- 604 at an Arctic polygonal tundra site: mathematical modelling with ecosys, J Geophys Res
- 605 Biogeosci, 122, 3174–3187, 2017.
- 606 Harrison, R. B., Footen, P. W., and Strahm, B. D.: Deep soil horizons: contribution and
- 607 importance to soil carbon pools and in assessing whole-ecosystem response to management
- 608 and global change, For. Sci., 57, 67–76, 2011.
- 609 Hastie, T.: The elements of statistical learning: data mining, inference, and prediction, 2009.
- 610 Hill, T., Chocholek, M., and Clement, R.: The case for increasing the statistical power of eddy
- 611 covariance ecosystem studies: why, where and how?, Glob. Change Biol., 23, 2154–2165,
- 612 https://doi.org/10.1111/gcb.13547, 2017.
- 613 Hochreiter, S.: Long Short-term Memory, Neural Comput. MIT-Press, 1997.
- 614 Justice, C. O., Townshend, J. R. G., Vermote, E. F., Masuoka, E., Wolfe, R. E., Saleous, N.,
- 615 Roy, D. P., and Morisette, J. T.: An overview of MODIS Land data processing and product
- 616 status, Remote Sens. Environ., 83, 3–15, 2002.
- 617 Kaufman, S., Rosset, S., Perlich, C., and Stitelman, O.: Leakage in data mining: Formulation,
- 618 detection, and avoidance, ACM Trans. Knowl. Discov. Data, 6, 1–21,
- 619 https://doi.org/10.1145/2382577.2382579, 2012.
- 620 Ke, G., Meng, Q., Finley, T., Wang, T., Chen, W., Ma, W., Ye, Q., and Liu, T.-Y.: Lightgbm: A
- 621 highly efficient gradient boosting decision tree, Adv. Neural Inf. Process. Syst., 30, 2017.
- 622 de Klein, J. J. and van der Werf, A. K.: Balancing carbon sequestration and GHG emissions in a
- 623 constructed wetland, Ecol. Eng., 66, 36–42, 2014.
- 624 Knox, S. H., Dronova, I., Sturtevant, C., Oikawa, P. Y., Matthes, J. H., Verfaillie, J., and
- 625 Baldocchi, D.: Using digital camera and Landsat imagery with eddy covariance data to model
- 626 gross primary production in restored wetlands, Agric. For. Meteorol., 237, 233–245, 2017.
- Knox, S. H., Bansal, S., McNicol, G., Schafer, K., Sturtevant, C., Ueyama, M., Valach, A. C.,
- 628 Baldocchi, D., Delwiche, K., Desai, A. R., Euskirchen, E., Liu, J., Lohila, A., Malhotra, A.,
- 629 Melling, L., Riley, W., Runkle, B. R. K., Turner, J., Vargas, R., Zhu, Q., Alto, T., Fluet-Chouinard,
- E., Goeckede, M., Melton, J. R., Sonnentag, O., Vesala, T., Ward, E., Zhang, Z., Feron, S.,
- 631 Ouyang, Z., Alekseychik, P., Aurela, M., Bohrer, G., Campbell, D. I., Chen, J., Chu, H.,
- Dalmagro, H. J., Goodrich, J. P., Gottschalk, P., Hirano, T., Iwata, H., Jurasinski, G., Kang, M.,
- Koebsch, F., Mammarella, I., Nilsson, M. B., Ono, K., Peichl, M., Peltola, O., Ryu, Y., Sachs, T.,
- 634 Sakabe, A., Sparks, J. P., Tuittila, E., Vourlitis, G. L., Wong, G. X., Windham-Myers, L., Poulter,
- 635 B., and Jackson, R. B.: Identifying dominant environmental predictors of freshwater wetland





- 636 methane fluxes across diurnal to seasonal time scales, Glob. Change Biol., 27, 3582–3604,
- 637 https://doi.org/10.1111/gcb.15661, 2021.
- Kumar, A., Bhatia, A., Fagodiya, R. K., Malyan, S. K., and Meena, B. L.: Eddy covariance flux
- 639 tower: A promising technique for greenhouse gases measurement, Adv Plants Agric Res, 7,
- 640 337–340, 2017.
- 641 Laćan, I. and Resh, V. H.: A case study in integrated management: Sacramento-San Joaquin
- 642 Rivers and Delta of California, USA, Ecohydrol. Hydrobiol., 16, 215–228, 2016.
- 643 Lee, H., Calvin, K., Dasgupta, D., Krinner, G., Mukherji, A., Thorne, P., Trisos, C., Romero, J.,
- 644 Aldunce, P., and Barrett, K.: Climate change 2023: synthesis report. Contribution of working
- 645 groups I, II and III to the sixth assessment report of the intergovernmental panel on climate
- 646 change, The Australian National University, 2023.
- 647 Li, C.: The DNDC Model, in: Evaluation of Soil Organic Matter Models, edited by: Powlson, D.
- 648 S., Smith, P., and Smith, J. U., Springer Berlin Heidelberg, Berlin, Heidelberg, 263–267,
- 649 https://doi.org/10.1007/978-3-642-61094-3 20, 1996.
- 650 Lolu, A. J., Ahluwalia, A. S., Sidhu, M. C., Reshi, Z. A., and Mandotra, S. K.: Carbon
- 651 Sequestration and Storage by Wetlands: Implications in the Climate Change Scenario, in:
- 652 Restoration of Wetland Ecosystem: A Trajectory Towards a Sustainable Environment, edited by:
- 653 Upadhyay, A. K., Singh, R., and Singh, D. P., Springer Singapore, Singapore, 45–58,
- 654 https://doi.org/10.1007/978-981-13-7665-8_4, 2020.
- 655 López, D., Sepúlveda, M., and Vidal, G.: Phragmites australis and Schoenoplectus californicus
- 656 in constructed wetlands: Development and nutrient uptake, J. Soil Sci. Plant Nutr., 16, 763–777,
- 657 2016.
- 658 Lund, J., Hanak, E., Fleenor, W., Bennett, W., and Howitt, R.: Comparing futures for the
- 659 Sacramento, San Joaquin delta, Univ of California Press, 2010.
- 660 Mack, S. K., Lane, R. R., Deng, J., Morris, J. T., and Bauer, J. J.: Wetland carbon models:
- 661 Applications for wetland carbon commercialization, Ecol. Model., 476, 110228, 2023.
- Matthes, J. H., Sturtevant, C., Oikawa, P., Chamberlain, S. D., Szutu, D., Arias-Ortiz, A.,
- 663 Verfaillie, J., and Baldocchi, D.: AmeriFlux AmeriFlux US-Myb Mayberry Wetland, Lawrence
- Berkeley National Laboratory (LBNL), Berkeley, CA (United States ..., 2016.
- Meyer, H. and Pebesma, E.: Machine learning-based global maps of ecological variables and
- the challenge of assessing them, Nat. Commun., 13, 2208, 2022.
- 667 Miller, R. L., Fram, M., Fujii, R., and Wheeler, G.: Subsidence reversal in a re-established
- 668 wetland in the Sacramento-San Joaquin Delta, California, USA, San Franc. Estuary Watershed
- 669 Sci., 6, 2008.
- 670 Mitsch, W. J. and Gosselink, J. G.: Wetlands, John wiley & sons, 2015.
- 671 Mitsch, W. J., Bernal, B., Nahlik, A. M., Mander, Ü., Zhang, L., Anderson, C. J., Jørgensen, S.
- E., and Brix, H.: Wetlands, carbon, and climate change, Landsc. Ecol., 28, 583–597, 2013.





- 673 Moomaw, W. R., Chmura, G. L., Davies, G. T., Finlayson, C. M., Middleton, B. A., Natali, S. M.,
- 674 Perry, J. E., Roulet, N., and Sutton-Grier, A. E.: Wetlands In a Changing Climate: Science,
- 675 Policy and Management, Wetlands, 38, 183–205, https://doi.org/10.1007/s13157-018-1023-8,
- 676 2018
- 677 Nahlik, A. M. and Fennessy, M. S.: Carbon storage in US wetlands, Nat. Commun., 7, 1–9,
- 678 2016.
- 679 Nelson, J. A., Walther, S., Gans, F., Kraft, B., Weber, U., Novick, K., Buchmann, N.,
- 680 Migliavacca, M., Wohlfahrt, G., and Šigut, L.: X-BASE: the first terrestrial carbon and water flux
- 681 products from an extended data-driven scaling framework, FLUXCOM-X, Biogeosciences, 21,
- 682 5079–5115, 2024.
- 683 Novick, K. A., Biederman, J. A., Desai, A. R., Litvak, M. E., Moore, D. J., Scott, R. L., and Torn,
- 684 M. S.: The AmeriFlux network: A coalition of the willing, Agric. For. Meteorol., 249, 444–456,
- 685 2018.
- 686 Oh, M., Lee, J., Kim, J., and Kim, H.: Machine learning-based statistical downscaling of wind
- resource maps using multi-resolution topographical data, Wind Energy, 25, 1121–1141,
- 688 https://doi.org/10.1002/we.2718, 2022.
- 689 Ouyang, Z., Jackson, R. B., McNicol, G., Fluet-Chouinard, E., Runkle, B. R., Papale, D., Knox,
- 690 S. H., Cooley, S., Delwiche, K. B., and Feron, S.: Paddy rice methane emissions across
- 691 Monsoon Asia, Remote Sens. Environ., 284, 113335, 2023.
- 692 Parton, W. J., Hartman, M., Ojima, D., and Schimel, D.: DAYCENT and its land surface
- submodel: description and testing, Glob. Planet. Change, 19, 35–48, 1998.
- 694 Pastorello, G., Trotta, C., Canfora, E., Chu, H., Christianson, D., Cheah, Y.-W., Poindexter, C.,
- 695 Chen, J., Elbashandy, A., and Humphrey, M.: The FLUXNET2015 dataset and the ONEFlux
- 696 processing pipeline for eddy covariance data, Sci. Data, 7, 225, 2020.
- 697 Peltola, O., Vesala, T., Gao, Y., Räty, O., Alekseychik, P., Aurela, M., Chojnicki, B., Desai, A.
- 698 R., Dolman, A. J., and Euskirchen, E. S.: Monthly gridded data product of northern wetland
- 699 methane emissions based on upscaling eddy covariance observations, Earth Syst. Sci. Data,
- 700 11, 1263–1289, 2019.
- 701 Perry, G. L. W., Seidl, R., Bellvé, A. M., and Rammer, W.: An Outlook for Deep Learning in
- 702 Ecosystem Science, Ecosystems, 25, 1700–1718, https://doi.org/10.1007/s10021-022-00789-y,
- 703 2022.
- 704 Raissi, M., Perdikaris, P., and Karniadakis, G. E.; Physics-informed neural networks; A deep
- 705 learning framework for solving forward and inverse problems involving nonlinear partial
- differential equations, J. Comput. Phys., 378, 686–707, 2019.
- 707 Räsänen, A., Manninen, T., Korkiakoski, M., Lohila, A., and Virtanen, T.: Predicting catchment-
- 708 scale methane fluxes with multi-source remote sensing, Landsc. Ecol., 36, 1177–1195,
- 709 https://doi.org/10.1007/s10980-021-01194-x, 2021.
- 710 Rey-Sanchez, C., Wharton, S., Vilà-Guerau De Arellano, J., Paw U, K. T., Hemes, K. S.,
- 711 Fuentes, J. D., Osuna, J., Szutu, D., Ribeiro, J. V., Verfaillie, J., and Baldocchi, D.: Evaluation of





- 712 Atmospheric Boundary Layer Height From Wind Profiling Radar and Slab Models and Its
- 713 Responses to Seasonality of Land Cover, Subsidence, and Advection, J. Geophys. Res.
- 714 Atmospheres, 126, e2020JD033775, https://doi.org/10.1029/2020JD033775, 2021.
- 715 Saunois, M., Martinez, A., Poulter, B., Zhang, Z., Raymond, P., Regnier, P., Canadell, J. G.,
- 716 Jackson, R. B., Patra, P. K., and Bousquet, P.: Global Methane Budget 2000–2020, Earth Syst.
- 717 Sci. Data Discuss., 2024, 1–147, 2024.
- 718 Sharma, S. and Singh, P.: Wetlands conservation: Current challenges and future strategies,
- 719 John Wiley & Sons, 2021.
- 720 Stewart, G. A., Sharp, S. J., Taylor, A. K., Williams, M. R., and Palmer, M. A.: High spatial
- 721 variability in wetland methane fluxes is tied to vegetation patch types, Biogeochemistry,
- 722 https://doi.org/10.1007/s10533-024-01188-2, 2024.
- 723 Tashman, L. J.: Out-of-sample tests of forecasting accuracy: an analysis and review, Int. J.
- 724 Forecast., 16, 437–450, 2000.
- 725 Tramontana, G., Jung, M., Schwalm, C. R., Ichii, K., Camps-Valls, G., Ráduly, B., Reichstein,
- 726 M., Arain, M. A., Cescatti, A., and Kiely, G.: Predicting carbon dioxide and energy fluxes across
- 727 global FLUXNET sites with regression algorithms, Biogeosciences, 13, 4291–4313, 2016.
- 728 Uhran, B. R., Windham-Myers, L., Bliss, N. B., Nahlik, A., Sundquist, E. T., and Stagg, C. L.:
- 729 Harmonizing wetland soil organic carbon datasets to improve spatial representation of 2011 soil
- 730 carbon stocks in the conterminous United States, https://doi.org/10.5066/P9H1PIX3, 2022.
- 731 Upadhyay, A. K., Singh, R., and Singh, D. P. (Eds.): Restoration of Wetland Ecosystem: A
- 732 Trajectory Towards a Sustainable Environment, Springer Singapore, Singapore,
- 733 https://doi.org/10.1007/978-981-13-7665-8, 2020.
- 734 Valach, A., Shortt, R., Szutu, D., Eichelmann, E., Knox, S., Hemes, K., Verfaillie, J., and
- 735 Baldocchi, D.: AmeriFlux AmeriFlux US-Tw1 Twitchell Wetland West Pond, Lawrence Berkeley
- 736 National Laboratory (LBNL), Berkeley, CA (United States ..., 2016.
- 737 Vaswani, A.: Attention is all you need, Adv. Neural Inf. Process. Syst., 2017.
- 738 Villa, J. A. and Bernal, B.: Carbon sequestration in wetlands, from science to practice: An
- 739 overview of the biogeochemical process, measurement methods, and policy framework, Ecol.
- 740 Eng., 114, 115–128, 2018.
- 741 Weiler, D. A., Tornquist, C. G., Zschornack, T., Ogle, S. M., Carlos, F. S., and Bayer, C.:
- 742 Daycent simulation of methane emissions, grain yield, and soil organic carbon in a subtropical
- 743 paddy rice system, Rev. Bras. Ciênc. Solo, 42, e0170251, 2018.
- 744 Windham-Myers, L., Bergamaschi, B., Anderson, F., Knox, S., Miller, R., and Fujii, R.: Potential
- 745 for negative emissions of greenhouse gases (CO2, CH4 and N2O) through coastal peatland re-
- establishment: Novel insights from high frequency flux data at meter and kilometer scales,
- 747 Environ. Res. Lett., 13, 045005, 2018.
- 748 Wood, D. A.: Machine learning and regression analysis reveal different patterns of influence on
- 749 net ecosystem exchange at two conifer woodland sites, Res. Ecol., 4, 24–50, 2022.





- 750 Workgroup, C. W. M.: EcoAtlas, 2019.
- 751 Xu, X. and Trugman, A. T.: Trait-Based Modeling of Terrestrial Ecosystems: Advances and
- 752 Challenges Under Global Change, Curr. Clim. Change Rep., 7, 1–13,
- 753 https://doi.org/10.1007/s40641-020-00168-6, 2021.
- 754 Xu, Y., Liu, X., Cao, X., Huang, C., Liu, E., Qian, S., Liu, X., Wu, Y., Dong, F., and Qiu, C.-W.:
- 755 Artificial intelligence: A powerful paradigm for scientific research, The Innovation, 2, 2021.
- 756 Yao, S., Chen, C., Chen, Q., Zhang, J., and He, M.: Combining process-based model and
- 757 machine learning to predict hydrological regimes in floodplain wetlands under climate change, J.
- 758 Hydrol., 626, 130193, 2023.
- 759 Yin, X., Jiang, C., Xu, S., Yu, X., Yin, X., Wang, J., Maihaiti, M., Wang, C., Zheng, X., and
- 760 Zhuang, X.: Greenhouse gases emissions of constructed wetlands: mechanisms and affecting
- 761 factors, Water, 15, 2871, 2023.
- 762 Yuan, K., Zhu, Q., Li, F., Riley, W. J., Torn, M., Chu, H., McNicol, G., Chen, M., Knox, S., and
- 763 Delwiche, K.: Causality guided machine learning model on wetland CH4 emissions across
- 764 global wetlands, Agric. For. Meteorol., 324, 109115, 2022.
- Yuan, K., Li, F., McNicol, G., Chen, M., Hoyt, A., Knox, S., Riley, W. J., Jackson, R., and Zhu,
- 766 Q.: Boreal–Arctic wetland methane emissions modulated by warming and vegetation activity,
- 767 Nat. Clim. Change, 14, 282–288, 2024.
- 768 Zhang, Y., Li, C., Trettin, C. C., Li, H., and Sun, G.: An integrated model of soil, hydrology, and
- 769 vegetation for carbon dynamics in wetland ecosystems, Glob. Biogeochem. Cycles, 16,
- 770 https://doi.org/10.1029/2001GB001838, 2002.
- 771 Zou, H., Chen, J., Li, X., Abraha, M., Zhao, X., and Tang, J.: Modeling net ecosystem exchange
- of CO2 with gated recurrent unit neural networks, Agric. For. Meteorol., 350, 109985, 2024.

774

775

776

777

778

779

780

781